

Probing space plasma with LOFAR

M. Grzesiak, Mariusz Pożoga, Barbara Matyjasiak, Dorota Przepiórka,
Hanna Rothkaehl, Katarzyna Budzińska, and Barbara Atamaniuk

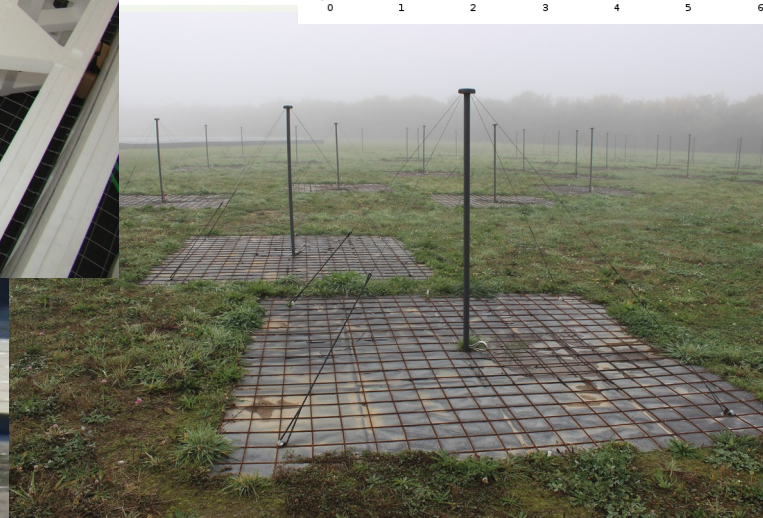
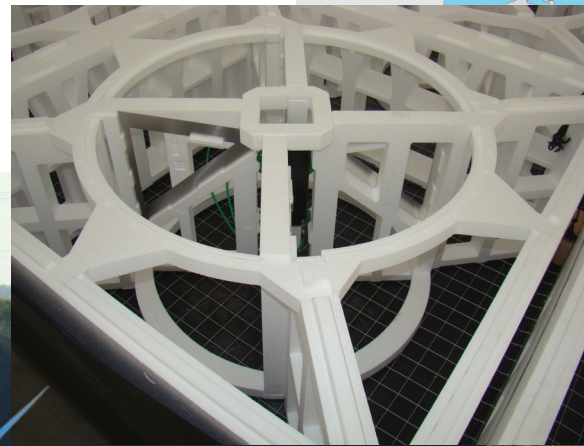
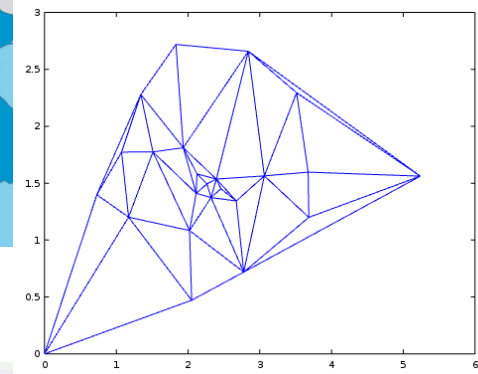
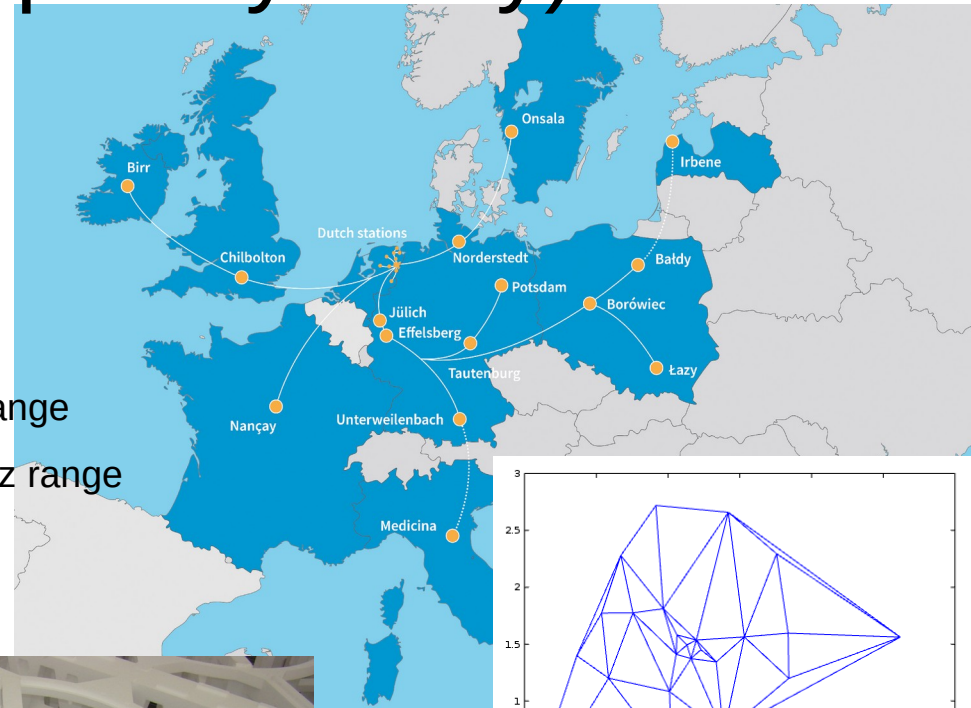
Space Climate Symposium,
Kraków, 2022

LOFAR (Low Frequency Array)

Interferometry in low frequencies (10-240 MHz)

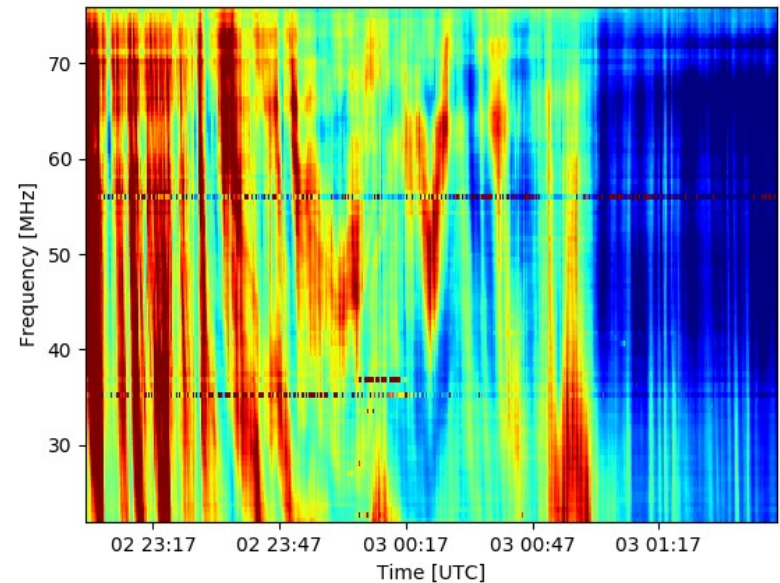
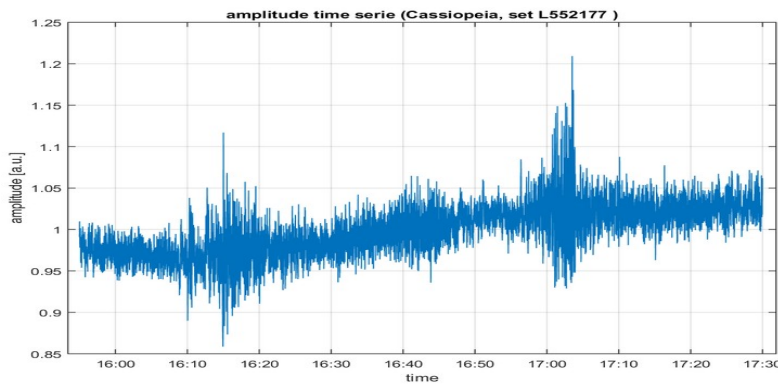
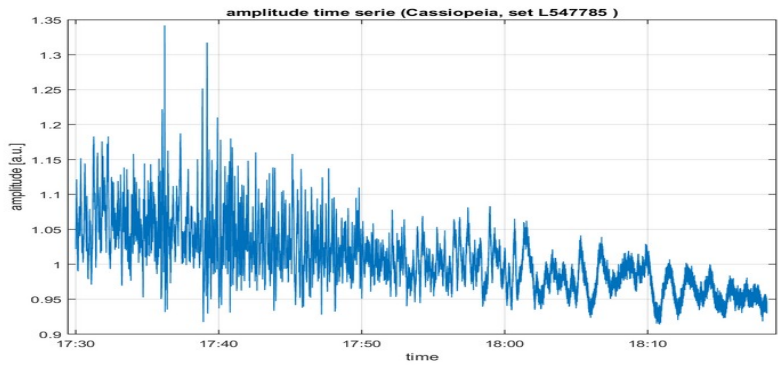
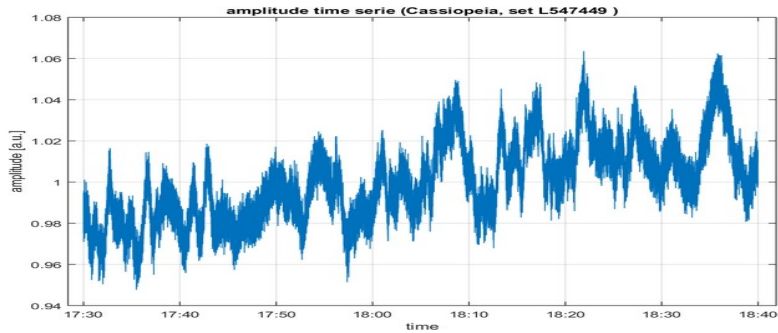
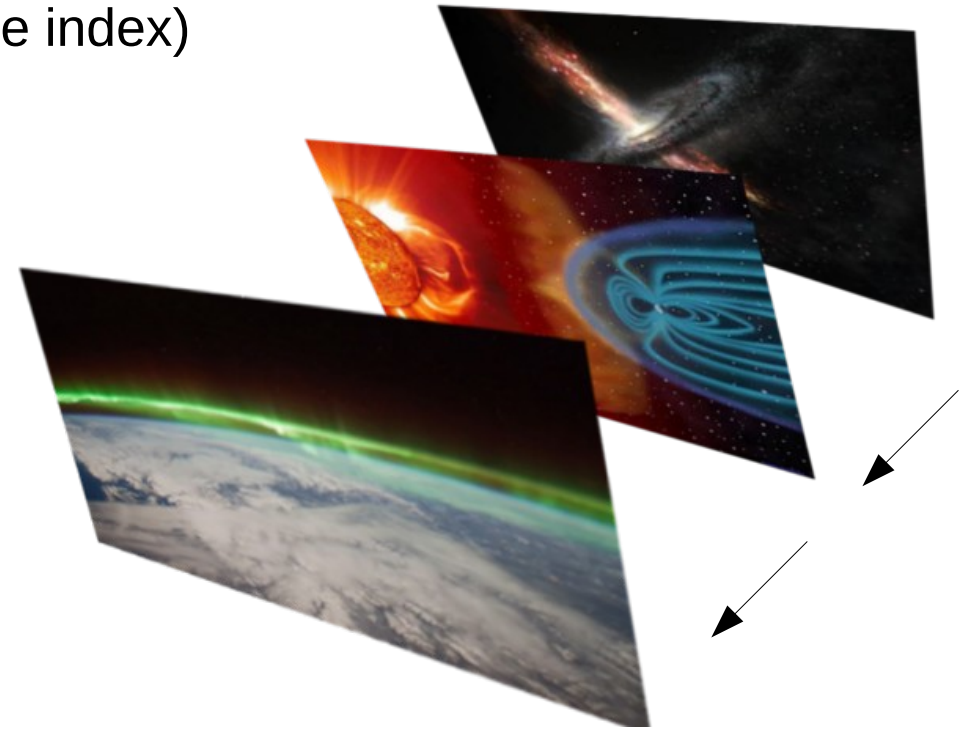
Consists of:

- Two antenna fields with 96 dipole antennas in each
- LBA (Low Band Antenna) – observations in 10-90 MHz range
- HBA (High Band Antenna) – observations in 110-240 MHz range
- Directional observations possible (beamforming)

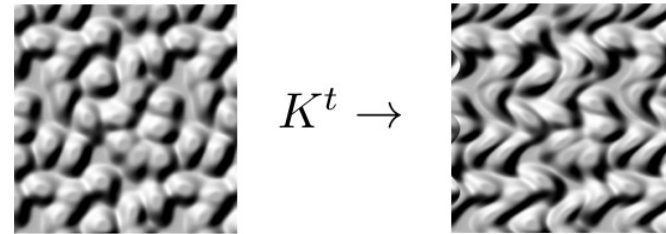
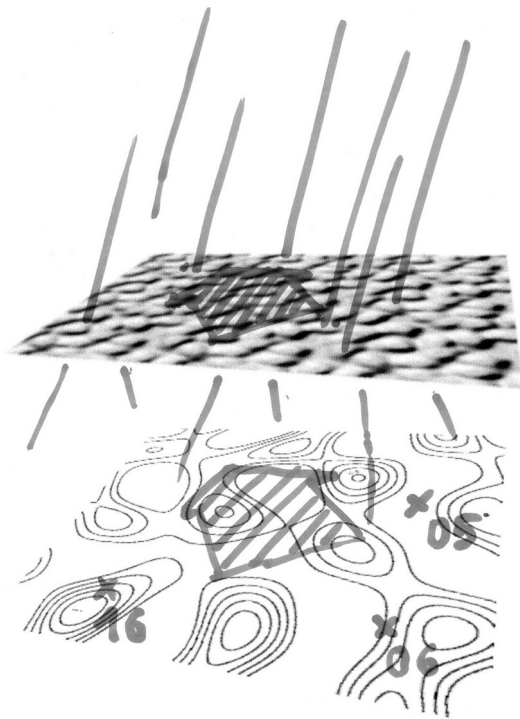


Scintillation

(fluctuations of wave characteristics after passing through medium with variable refractive index)



Modeling pattern evolution – dispersion analysis



$$\psi(\mathbf{r}, t) = \int d\mathbf{r}' K^t(\mathbf{r} - \mathbf{r}') \psi(\mathbf{r}', 0)$$

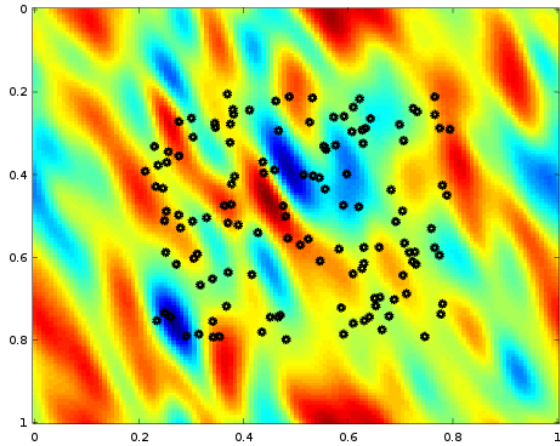
$$\hat{\psi}(\mathbf{k}, t) = \hat{\psi}(\mathbf{k}, 0) e^{\Omega(\mathbf{k})t}$$

$$\mathbb{E}[\psi(\mathbf{r}_1, t_1) \psi(\mathbf{r}_2, t_2)] = \int d\mathbf{k} P(\mathbf{k}) e^{\Omega(\mathbf{k})\tau} e^{i\mathbf{k} \cdot \boldsymbol{\zeta}} = C(\boldsymbol{\zeta}, \tau),$$

$$\boldsymbol{\zeta} = \mathbf{r}_2 - \mathbf{r}_1, \tau = t_2 - t_1$$

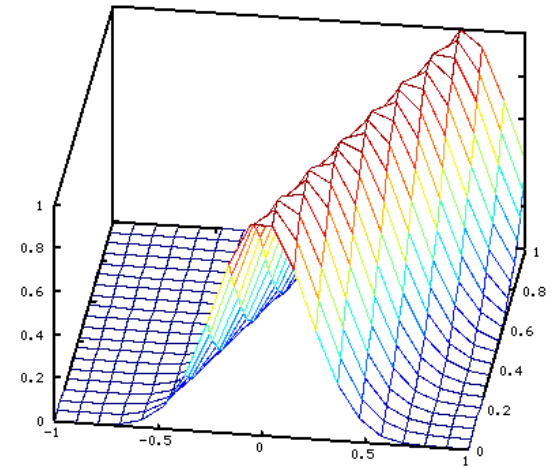
$$\langle \boldsymbol{\zeta} \rangle = \frac{\int d\boldsymbol{\zeta} \boldsymbol{\zeta} C(\boldsymbol{\zeta}, \tau)}{\int d\boldsymbol{\zeta} C(\boldsymbol{\zeta}, \tau)} \quad \frac{\partial}{\partial \tau} \langle \boldsymbol{\zeta} \rangle = \nabla_{\mathbf{k}} \Omega(\mathbf{k})|_{\mathbf{k}=0}$$

Basic example – rigid motion



$$K(\mathbf{r}' - \mathbf{r}, t) = \delta(\mathbf{r}' - (\mathbf{r} - \mathbf{v}dt))$$

$$\frac{\partial}{\partial t} C - \mathbf{v} \cdot \nabla_{\xi} C = 0$$



$$\xi_{\alpha} = \mathbf{r}_k - \mathbf{r}_l$$

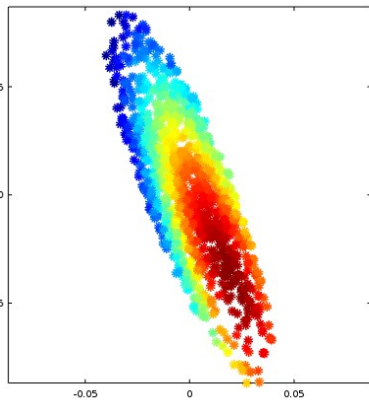
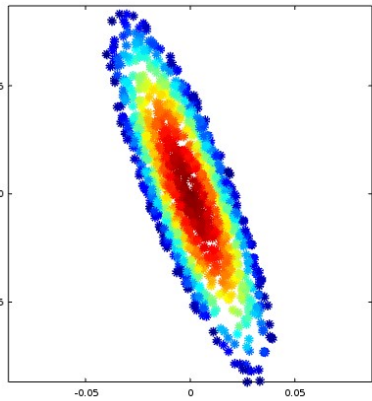
Simulation

Example from LOFAR

$$\tau_{\alpha} = 0$$

<

$$\tau_{\alpha}$$



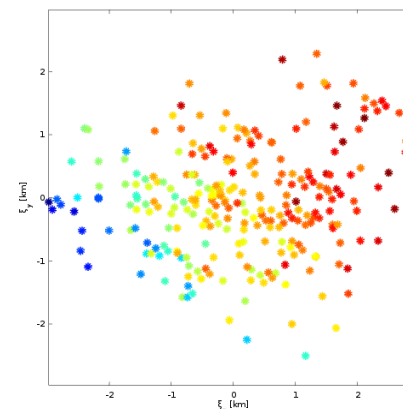
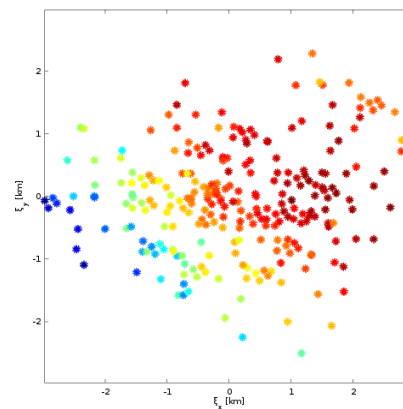
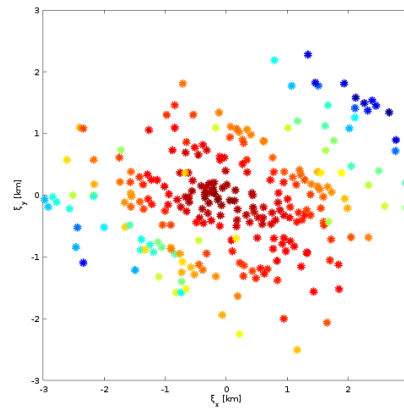
$$\tau_{\alpha} = 0$$

<

$$\tau_{\alpha}$$

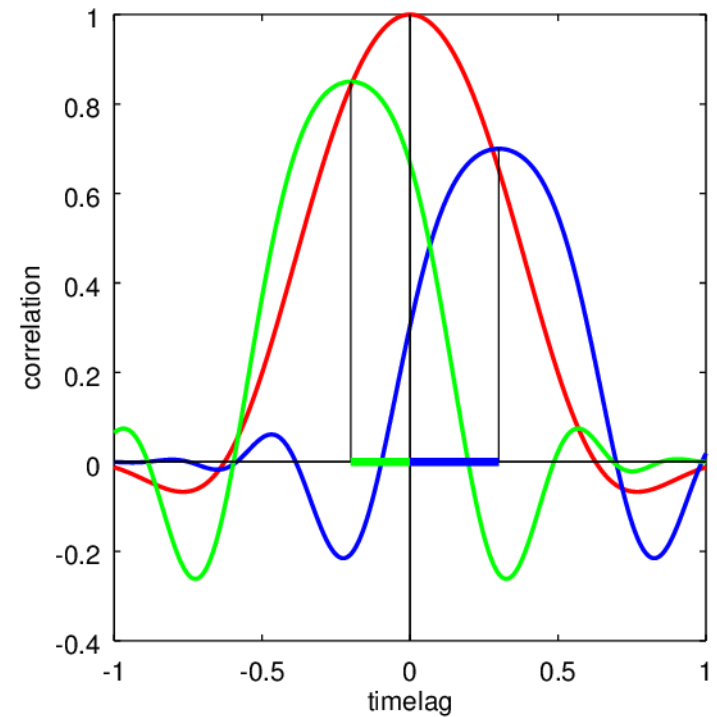
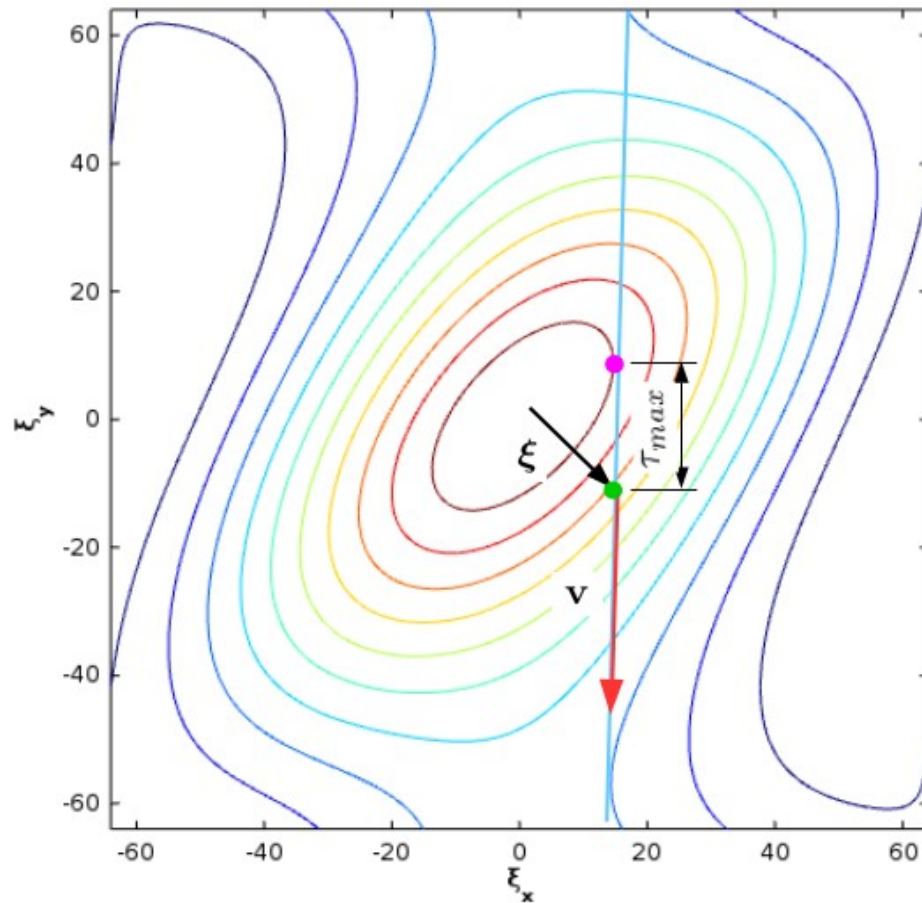
<

$$\tau_{\alpha}$$



Correlation function features recognition

$$C(\xi - \mathbf{v}\tau)$$



Briggs, B. H., On the analysis of moving patterns in geophysics, I, Correlation analysis, J. Atmos. Terr. Phys., 30, 1777-1788, 1968.

Estimation of geometry and drift velocity

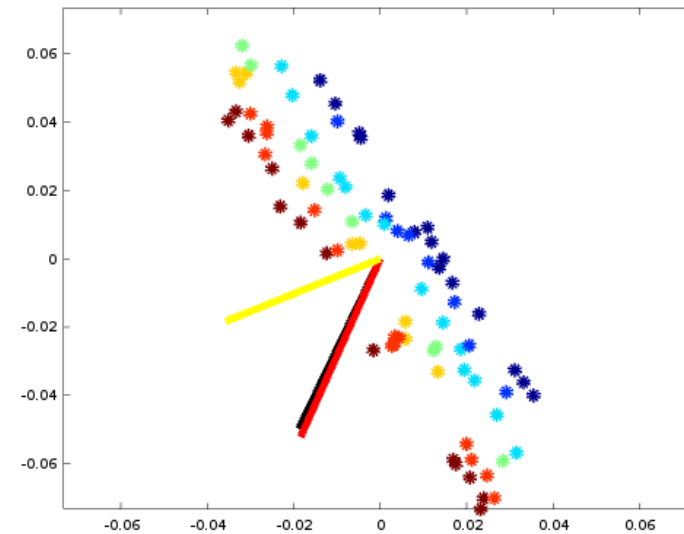
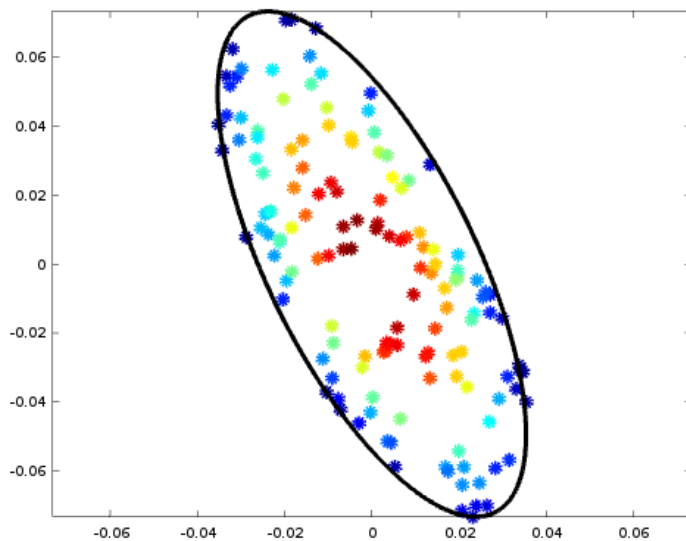
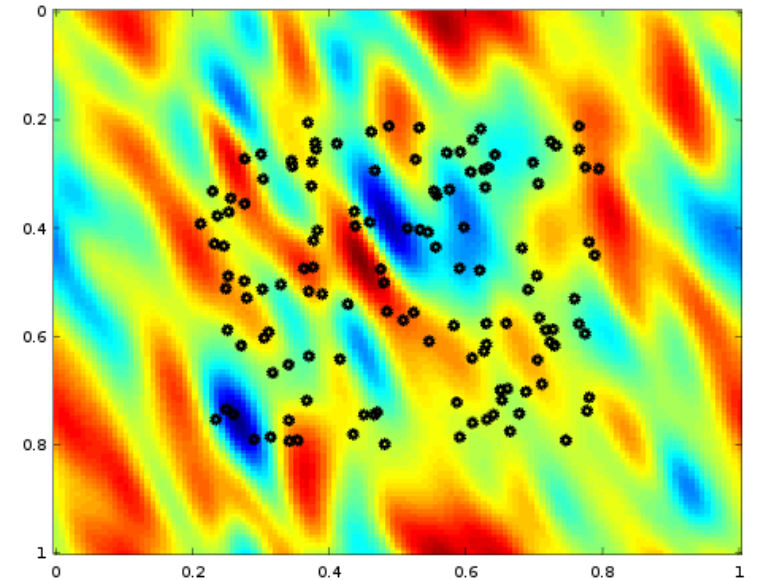
$$C(\boldsymbol{\xi}) = \rho(\boldsymbol{\xi}^T Q \boldsymbol{\xi})$$

$$\frac{\partial}{\partial \tau} C(\boldsymbol{\xi} - \mathbf{v}\tau) = 0$$

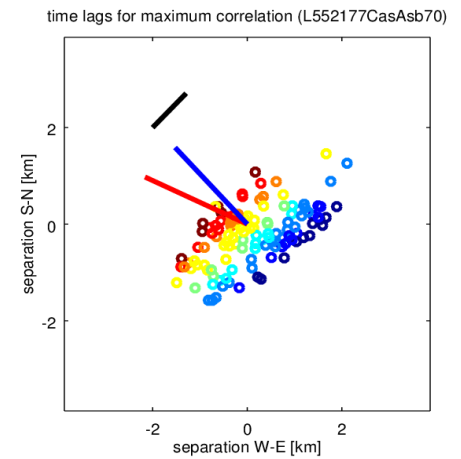
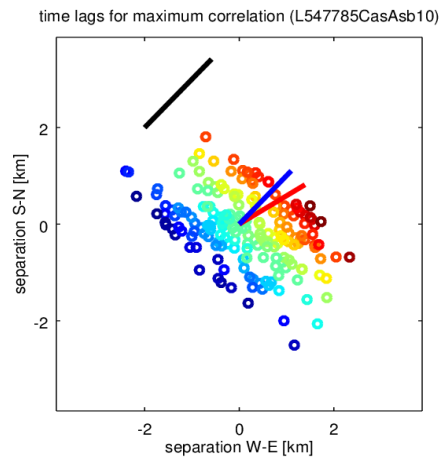
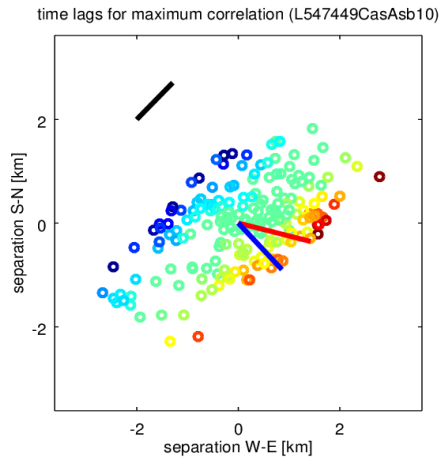
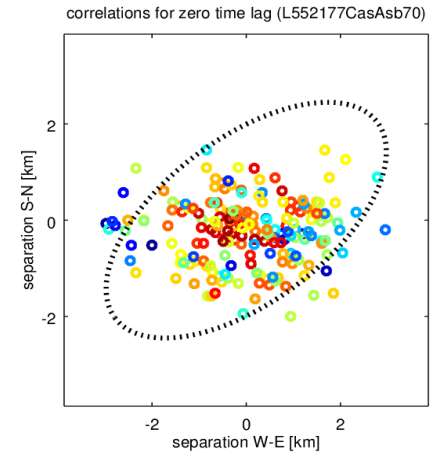
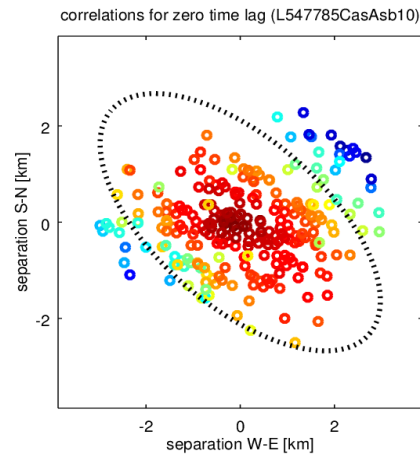
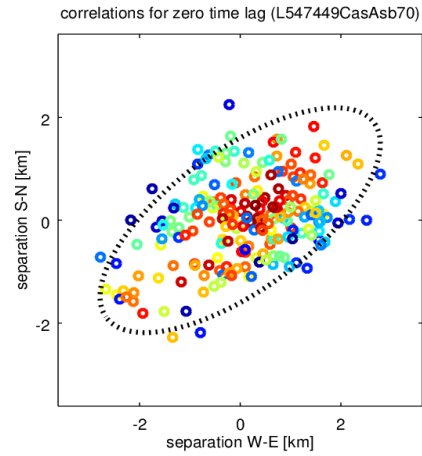
$$\boldsymbol{\xi}^T Q \mathbf{v} = \tau_m \mathbf{v}^T Q \mathbf{v} \rightarrow \tau_m = \frac{\boldsymbol{\xi}^T Q \mathbf{v}}{\mathbf{v}^T Q \mathbf{v}}$$

$$\nabla_{\boldsymbol{\xi}} \tau_m = \frac{Q \mathbf{v}}{\mathbf{v}^T Q \mathbf{v}}$$

$$\mathbf{v} = \frac{Q^{-1} \nabla_{\boldsymbol{\xi}} \tau_m}{(\nabla_{\boldsymbol{\xi}} \tau_m)^T Q^{-1} \nabla_{\boldsymbol{\xi}} \tau_m}$$

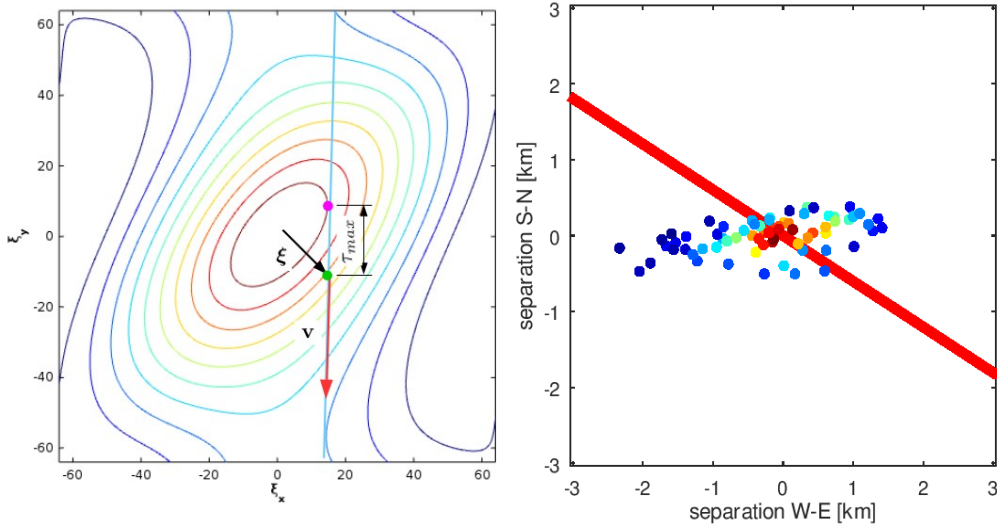


Estimation of geometry and drift velocity



data set	v_x [m/s]	v_y [m/s]	magnitude [m/s]	v_x isotropic [m/s]	v_y isotropic [m/s]	magnitude isotropic [m/s]
L547449	142	-35	147	86	-90	124
L547785	694	408	804	549	552	778
L552177	-2160	795	2370	-1526	1586	2200

Testing the frozen flow hypothesis



Let us create a quantitative comparison between spatial and temporal correlations by putting the origin of our new coordinate system at ζ and make the substitution $\tau \rightarrow \mathbf{v}\tau$. We took the spatial correlations at points close to the forementioned line and plot both: spatial correlation and temporal cross-correlation at the same figure 1 – clearly they do not overlap. Then rescaling: $\tau \rightarrow \gamma\mathbf{v}\tau$ we try to find the best fit by minimising:

$$\min_{\gamma} \sum_k (C_s(\zeta_k) - C_t(\gamma\mathbf{v}\tau_k))^2$$

where **s** stands for spatial and **t** temporal correlations.

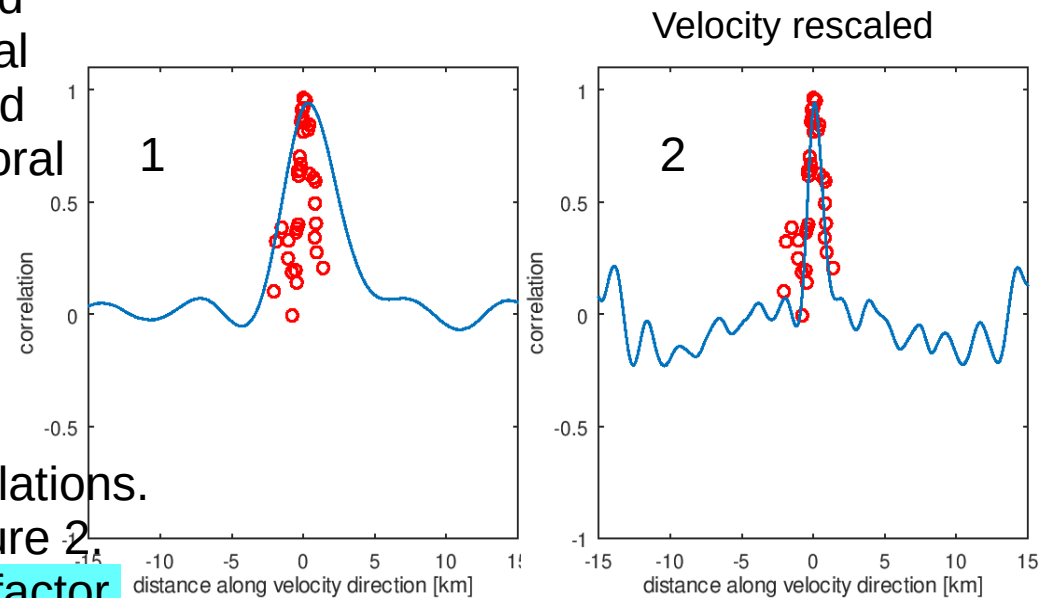
The result of the procedure is shown in the figure 2

The γ can be considered as a velocity scaling factor.

Recall the relationship between purely spatial correlation and the cross-correlation at two different locations in the frozen flow model:

$$\begin{cases} \langle \psi(\mathbf{r}_1, t_1) \psi(\mathbf{r}_2, t_2) \rangle = C(\zeta - \mathbf{v}\tau) \\ \zeta = \mathbf{r}_2 - \mathbf{r}_1, \tau = t_2 - t_1 \end{cases}$$

which means that temporal cross-correlation function for given pair of receivers is the cut of the spatial correlation function along the line $\zeta = \zeta_0 - \mathbf{v}\tau$, where ζ_0 is the actual spatial the displacement between receivers 1 and 2.



The temporal decorrelation

The possible cause for this velocity overestimation was pointed out by Briggs (1968) in the exposition of his full correlation analysis. The additional temporal decorrelation may lead to overestimation of the velocity when using gradient of the timelag only. The picture below explains this effect: when additional temporal decorrelation is present the evolution of a field would be described by spatio-temporal quadratic form:

$$q(\zeta, \tau) = [\zeta \quad \tau] \begin{bmatrix} Q_s & 0 \\ 0 & \beta \end{bmatrix} \begin{bmatrix} \zeta \\ \tau \end{bmatrix} \quad 1$$

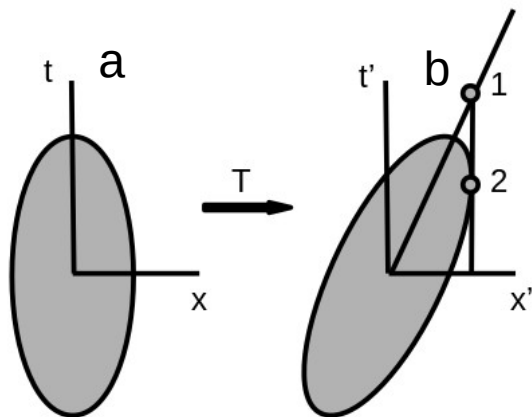
which describes also an elliptic shape of the isosurfaces of spatio-temporal correlation (figure a below). The Q_s is the spatial part of the full matrix while β describes temporal fading. When the field is moving with the velocity \mathbf{v} the matrix of the quadratic form transforms into:

$$Q' = T^T Q T \quad 2$$

what is shown in figure b. It also explains why the overestimation takes place: the timelag to maximum recognizes point 2 (as it is tangent to an isosurface) while correct position is at point 1.

Writing explicitly matrix T we can obtain the Q in new coordinate system, Q' :

$$T = \begin{bmatrix} 1 & 0 & v_x \\ 0 & 1 & v_y \\ 0 & 0 & 1 \end{bmatrix} = \begin{bmatrix} I & \mathbf{v} \\ \mathbf{0}^T & 1 \end{bmatrix} \quad Q' = \begin{bmatrix} Q_s & Q_s \mathbf{v} \\ \mathbf{v}^T Q_s & \beta + \mathbf{v}^T Q_s \mathbf{v} \end{bmatrix} \quad 3$$



If matrix can be transformed to the form as in 1 (block-diagonal) by the transformation T , we call it separable. It means that there exists a reference frame in which the pattern is at rest (possibly flickering).

An alternative method of drift estimation, the meaning of γ

Let us look at the Q' matrix:

$$Q' = \begin{bmatrix} Q_s & Q_s \mathbf{v} \\ \mathbf{v}^T Q_s & \beta + \mathbf{v}^T Q_s \mathbf{v} \end{bmatrix}$$

$Q'_{[1:2;3]}$

It allows for a new estimate of drift velocity:

$$\mathbf{v}_T = Q_s^{-1} Q'_{[1:2;3]}$$

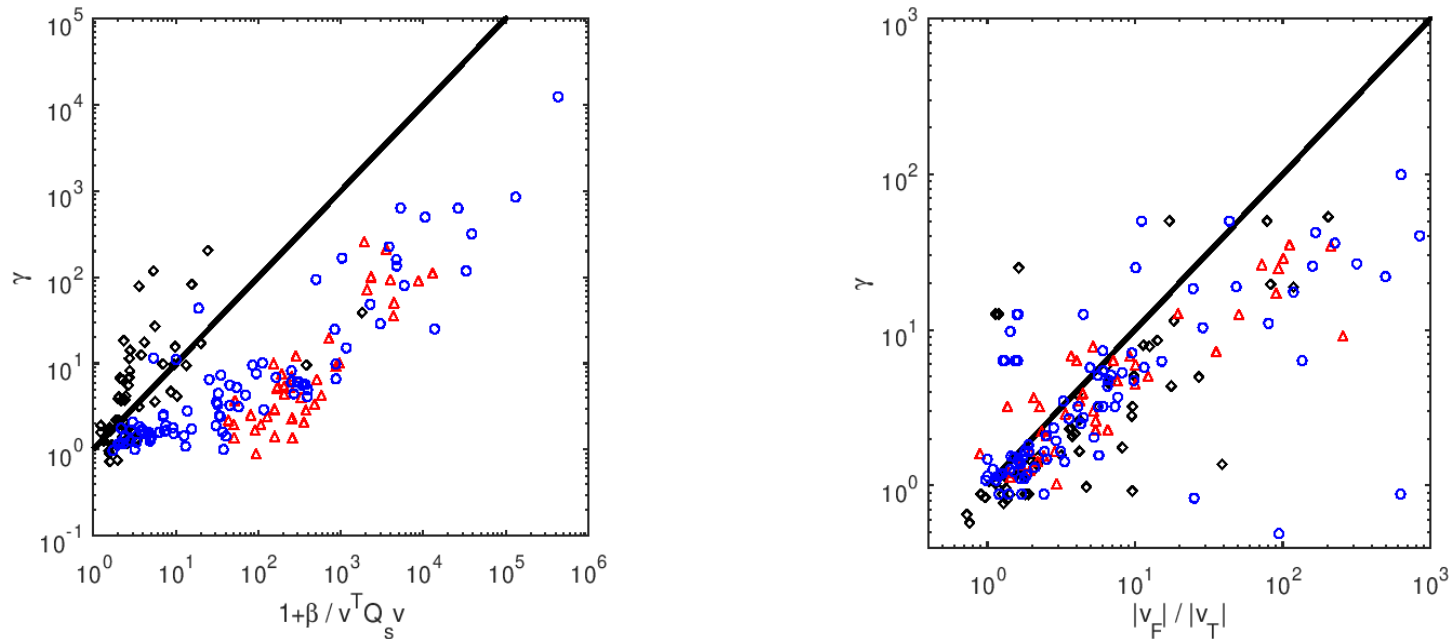
If we want to compare the frozen flow estimate \mathbf{v}_F with the defined above, using the same time-lag to the maximum of cross-correlation we arrive at:

$$\mathbf{v}_F = \left(1 + \beta / \mathbf{v}_T^T Q_s \mathbf{v}_T\right) \mathbf{v}_T$$

γ

So, this gives formally a possible explanation for the observed overestimation of the drift velocity – the faster fading / smaller actual drift velocity the stronger overestimation.

Using LOFAR scintillation measurements, we can check if estimated from the data γ follows the one anticipated by the model with temporal decorrelation. We took for Q' the fit of second order polynomial in three variables to the actual spatio-temporal correlation close to the origin to get both v_F and $1+\beta/v^T Q_s v$. The results are plotted below. Different markers refer to different data sets. Each data set has been divided into 3 mins. length overlapping intervals.

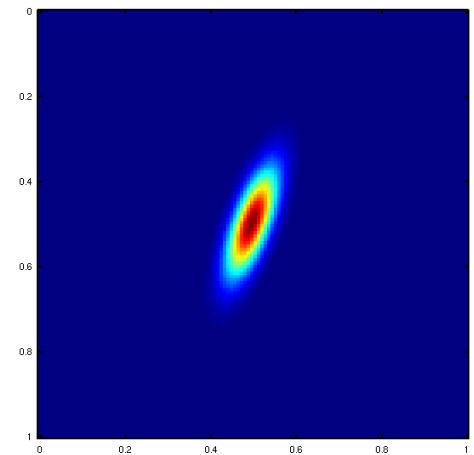
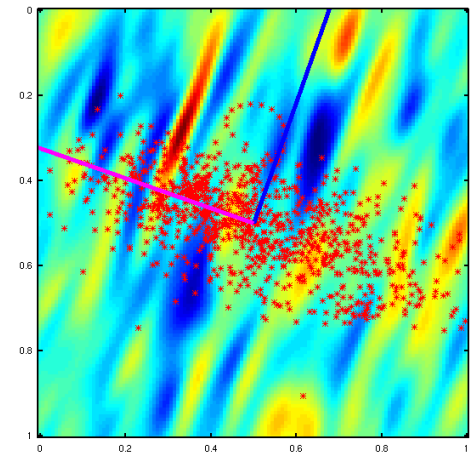
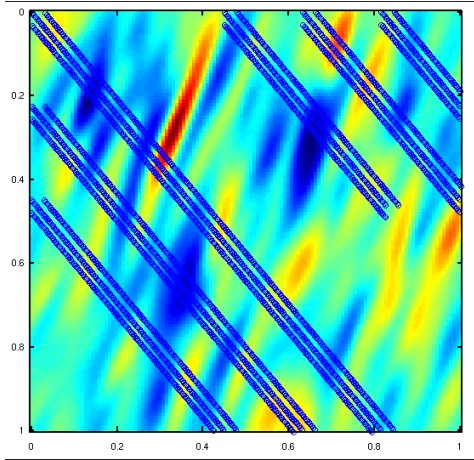


Clearly, v_F is more universal and gives closer to data velocity scaling than the drift + temporal decorrelation.

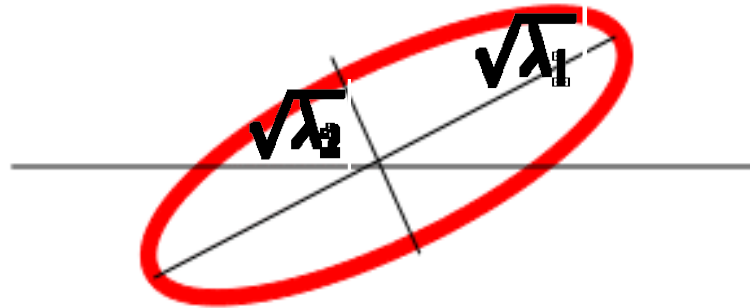
Structure reconstruction (2D case)

2D test field with satellites traces imposed

Gradients cloud and eigendirections of covariance matrix

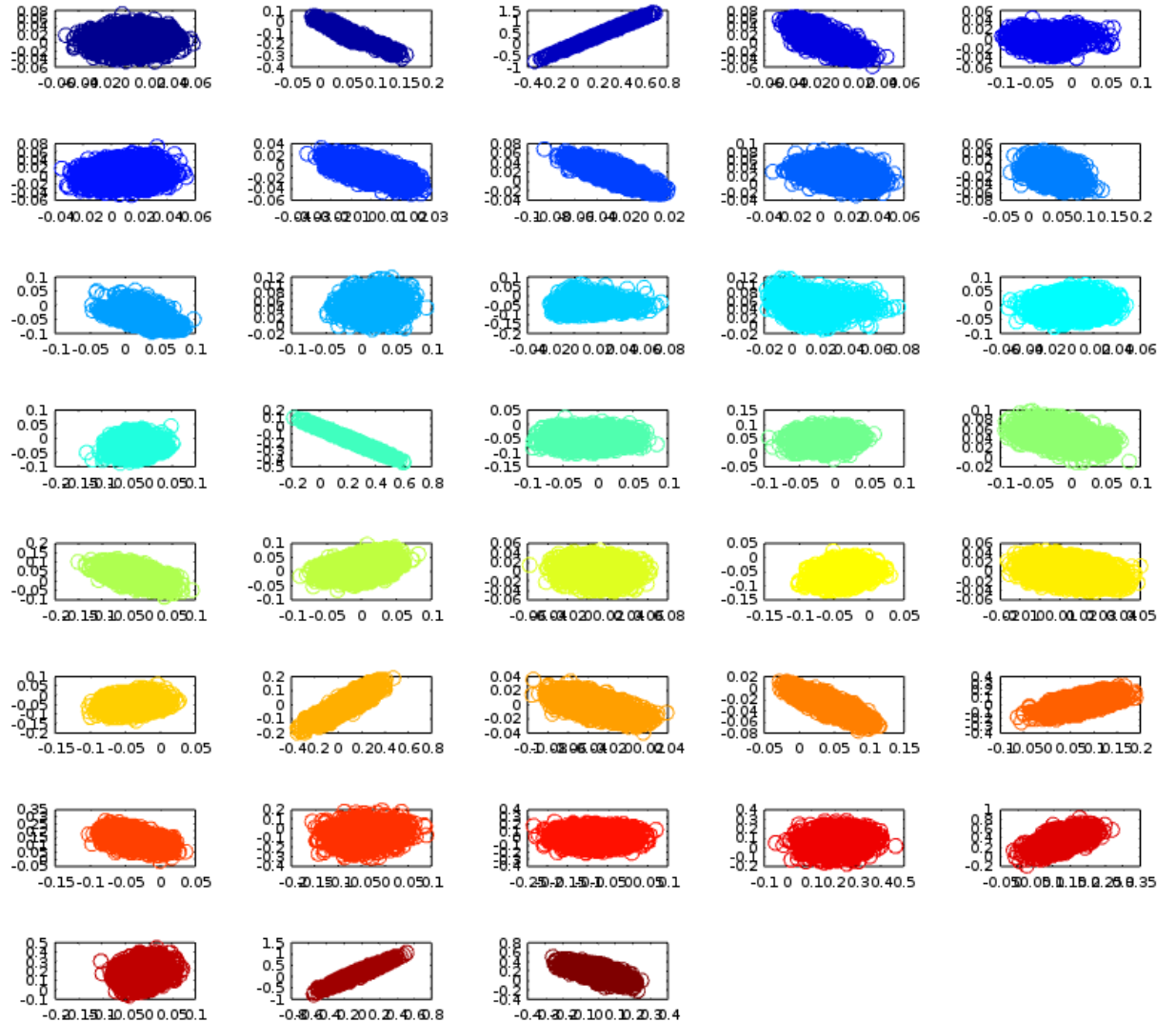
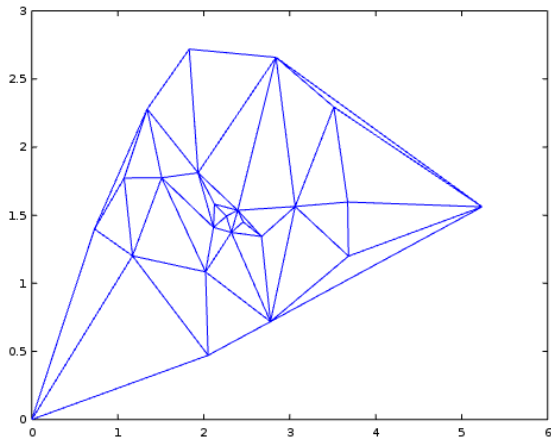


$$g_{kl} = \frac{1}{\mathbf{var}(f)} \left\langle \frac{\partial f}{\partial x_k} \frac{\partial f}{\partial x_l} \right\rangle = \frac{\int d\mathbf{k} k_k k_l P(\mathbf{k})}{\int d\mathbf{k} P(\mathbf{k})}$$

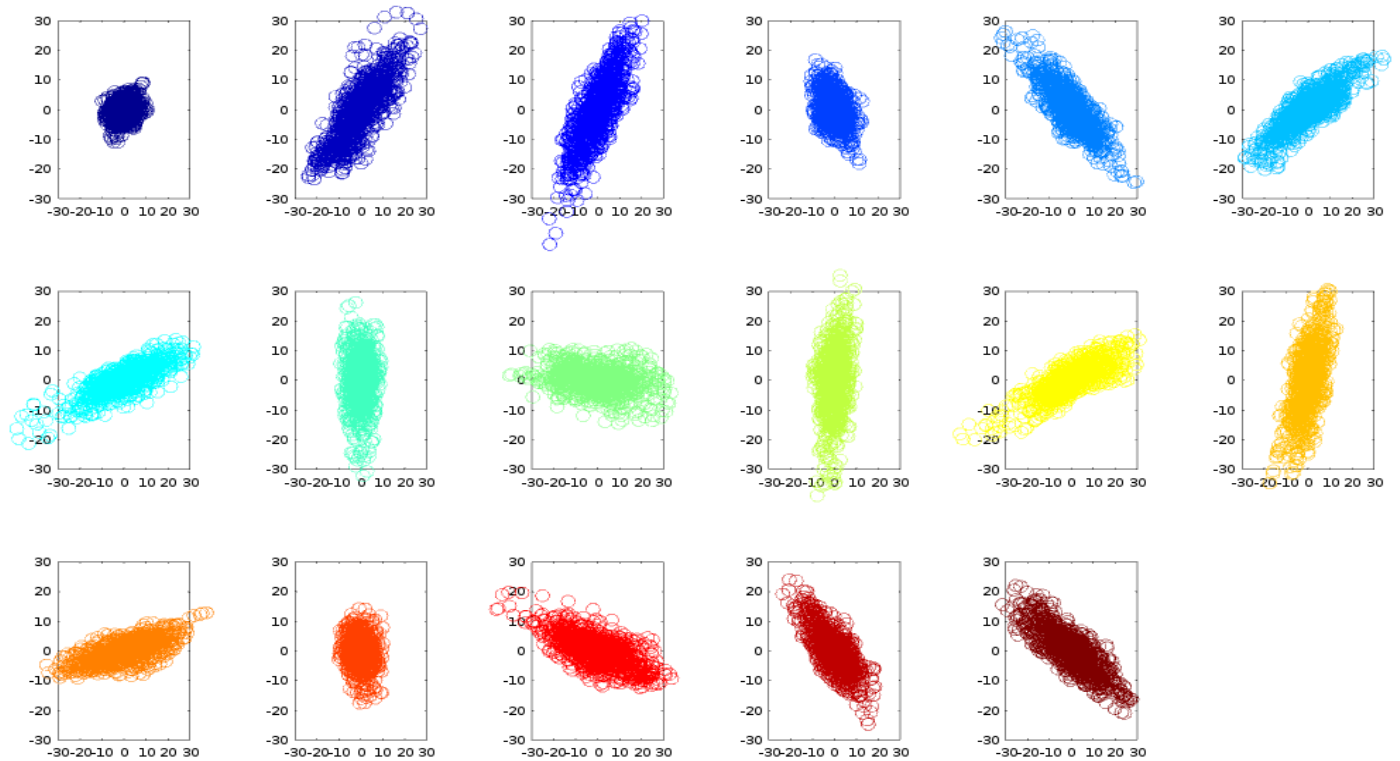
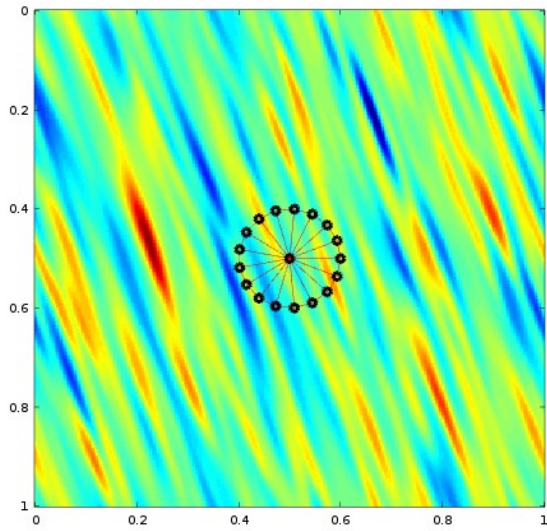


Reconstructed structure

Problems with geometry



Possible solution



Conclusions

LOFAR network provides consistent scintillation data of coverage both in time and space that equips us with new possibilities of spatio-temporal analysis.

The method presented gives estimate of drift velocity taking into account possible anisotropy of irregularities. It turns out that the magnitude of drift velocity depends on geomagnetic activity: the larger Kp index the greater velocity which is in agreement with previous observations.

For some conditions, the frozen flow assumption seems violated, and different velocity estimates are more suitable.